

The 2012 Australian Seismic Hazard Map – Draft Maps

David Burbidge and Mark Leonard

Geospatial & Earth Monitoring Division, Geoscience Australia,
Canberra ACT 2601, Australia

Corresponding Author: David.Burbidge@ga.gov.au

Abstract

This final paper for the session presents the results of the new draft earthquake hazard assessment for Australia and compares them to the previous AS1170.4 hazard values. Draft hazard maps will be presented for several response spectral acceleration (RSA) periods (0.0, 0.2 and 1.0 s) at multiple return periods (500, 2500 and 10,000 years). These maps will be compared with both the current earthquake hazard used in AS1170.4 and with other assessments of earthquake hazard in Australia. In general the hazard in the draft map is higher in the western, cratonic, parts of Australia than it is in the eastern, non-cratonic, parts of Australia. Where regional source zones are included, peaks in hazard values in the map are generally comparable (i.e. within $\sim 0.04g$) to those in the current AS1170.4 map. When seismicity 'hotspot' zones are included, as described in the previous paper, several of them produce much higher hazard peaks than any in the AS1170.4 map. However, such hotspots do not affect as large an area as many of those in the current AS1170.4 map. Finally, hazard curves for four different cities will also be presented and compared to those predicted by the method outlined in AS1170.4. For the locations examined, the hazard curves generated from AS1170.4-2007 are closest to either the 0.0 or 0.2 s RSA period hazard curves in the draft assessment depending on the location.

Introduction

The draft seismic hazard maps have been created using GA's open source earthquake hazard and risk model, EQRM. EQRM is available as a free download from <http://eqrm.sourceforge.net/>. EQRM is an event-based hazard and risk code in which a "synthetic catalogue" of events is generated across the region of interest to calculate the hazard or risk (Robinson *et al.* 2006). This event-based approach differs from that of a traditional probabilistic seismic hazard assessment (PSHA), which integrates over all magnitude and distance combinations to obtain the hazard. The event-based approach has the advantage of being easy to extend to risk (i.e. loss) maps, but is more computationally intensive. Further details regarding EQRM can be found in Robinson *et al.* (2005), Robinson *et al.* (2006) or the documentation which comes with the latest version of EQRM.

Method

The following steps are needed in order to calculate a seismic hazard map from a synthetic catalogue of earthquakes (Robinson *et al.* 2006)

1. a synthetic earthquake catalogue is generated from an earthquake source (or occurrence) model;
2. the level of ground shaking from each earthquake is propagated to the sites of interest using one or more attenuation models (also known as ground motion prediction equations - GMPEs);
3. the local regolith and its effect on ground shaking is then included using a site response model (if needed); and
4. the hazard is estimated by summing the probabilities of all events that exceed a particular ground motion for all the sites of interest.

Source location, magnitude and ground motion variability are taken into consideration by randomly sampling their respective probability density functions (PDFs) as described in Robinson *et al.* (2005). The ground motion equations used, and their respective weightings applied to represent the uncertainty in the choice of ground motion model, are described in Allen *et al.* (this volume).

For the draft hazard maps presented here the following parameters/models were applied:

1. Rupture planes were formed for each earthquake with a dip restricted to 35 degrees but with a free strike (i.e. they can be orientated any direction). Earthquakes were distributed in each zone with a spatial density of between 2 and 5 earthquakes per square kilometre depending on the map layer.
2. Dimensions of the rupture (i.e. length and width) for a given magnitude were taken from the Stable Continental Relations equations in Leonard (2010).
3. Earthquakes are evenly distributed in each zone between the surface and 15 km in depth.
4. The minimum magnitude considered for each zone is 4.5. The maximum magnitude and recurrence model for each zone is described in Leonard *et al.* (this volume).
5. Revised local magnitude (ML) values (Allen *et al.* this volume) were used to calculate the Gutenberg-Richter (G-R) values shown in this paper. The G-R values for the unrevised and moment magnitude versions of the catalogue were also calculated for comparison purposes but are not discussed here.
6. Ground motions were calculated out to a distance of 400 km for each earthquake.

7. The resulting probabilistic hazard maps were created at return periods of 500, 2475 and 10,000 years. The hazard values in these maps correspond to ground motions with (respectively) a 1/500, 1/2475 and 1/10,000 chance of being exceeded each year.
8. For each return period, the hazard values are calculated at response spectral accelerations (RSA) at periods of 0.0, 0.2 and 1.0 s. These three RSA periods were chosen as a result of consultation at the initial planning workshop (Burbidge *et al.* 2010). The 0.0 s map is also known as the “peak ground acceleration” hazard map.
9. No site amplification was applied (i.e. the ground motion was calculated for hard rock site conditions) to ensure it is consistent with the current map in AS1170.4 which is also set for these conditions. Similarly, the resulting seismic risk (i.e. the losses) from the hazard has not been calculated.

Note that some of these parameters are expected to be different for the final map, scheduled to be completed by mid-2012. For example, the final hazard assessment will have more return periods and the depth distribution will vary for each zone. We also intend to revise the GMPEs as discussed in Allen *et al.* (this volume). However, these changes are expected to have a relatively small impact, particularly on the 500 year return period maps, and the following preliminary results should provide a reasonable guide as to the final results.

To calculate the hazard, up to about 25 million earthquakes (depending on the layer) are generated synthetically and the ground motions are calculated for a set of 17,000 regularly spaced points across Australia for each earthquake. The points are arranged in a grid with a 0.2 degree spacing. Only points onshore mainland Australia and Tasmania are included. The ground motions at each point are then used to calculate the hazard at the various RSA periods required. Thus, for each of the 17,000 locations across Australia, we have nine hazard values (three RSA periods for three different return periods) for each layer. This data is saved as a series of GMT (Generic Mapping Tools, <http://gmt.soest.hawaii.edu/>) compatible NetCDF files. Standard GMT tools can then be used for post-processing. For example, the maximum of the background, regional and hotspot zones can be found using “grdmath” or the data can be smoothed with “grdfilter”. The data can also be interpolated using “grdtrack” to estimate the hazard for any given latitude and longitude in Australia. GMT tools are also used to generate maps to visualise the hazard values shown in the next section.

Results

As described in Leonard *et al.* (2011), this hazard assessment consists of a number of layers. In this section we present a range of different hazard maps for different layers, return periods and RSA periods, and show how these could be combined into a final hazard map. Each hazard map is also convolved with a 2D Gaussian function with a specified width. This has two effects:

1. the small detail in the maps which are smaller than the Gaussian width are removed. This reduces the level of detail, reduces numerical noise and produces a smoother final map;
2. the Gaussian function can be interpreted as representing the spatial uncertainty in the hazard (e.g. due to the imprecise location of the zone boundaries). The Gaussian width is 6 times the standard deviation. This means that convolving the hazard map with a 300 km width Gaussian function also implies that aspects such as the zone boundaries have effectively a spatial uncertainty of +/- 50 km at one standard deviation.

The smoothing has the effect of softening the hard edges produced by source zone based hazard maps. The effect is similar to weighting a large number of alternative zonation hazard maps where the boundary location varies spatially. The AS1170.4 map was also smoothed for similar reasons (i.e. to represent the spatial uncertainty to zone boundaries), as documented by McCue (1993). However, in this case the smoothing is done with an open source code and documented parameters.

Background Source Zones Only

Figure 1 shows the 500 yr, PGA (i.e. 0.0 s RSA period) hazard for the background zones only; a 300 km wide Gaussian spatial filter was used to smooth the map. The 0.0 s RSA period hazard in this map is everywhere low (i.e. < 0.05 g), but is higher in the cratonic and extended parts of Australia (west of the Tasman Line and in southern Victoria) than in the non-cratonic (eastern) areas of Australia. This is due to a combination of higher rate of earthquake occurrence and lower attenuation in the cratonic parts of Australia (Allen *et al.* this volume).

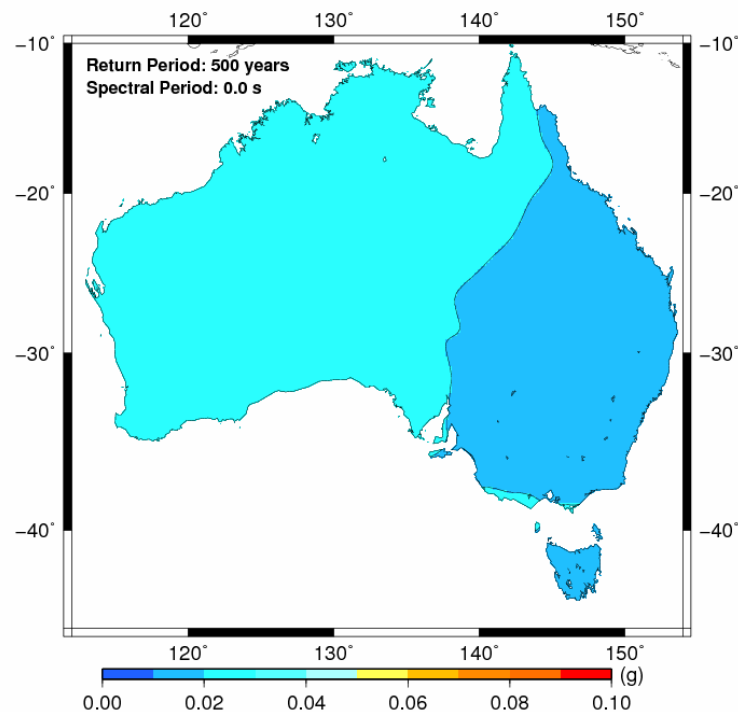


Figure 1 - The 500 year return period background zone PGA (0.0s RSA period) hazard map smoothed with a 300 km Gaussian spatial filter.

Regional Source Zones Only

Figure 2 shows the 500 yr, 0.0 s hazard for the regional zones only, smoothed with a 300 km width Gaussian filter. In a similar way to the background zones, hazard values tend to be higher in the western, cratonic parts of Australia than in the eastern non-cratonic areas of Australia.

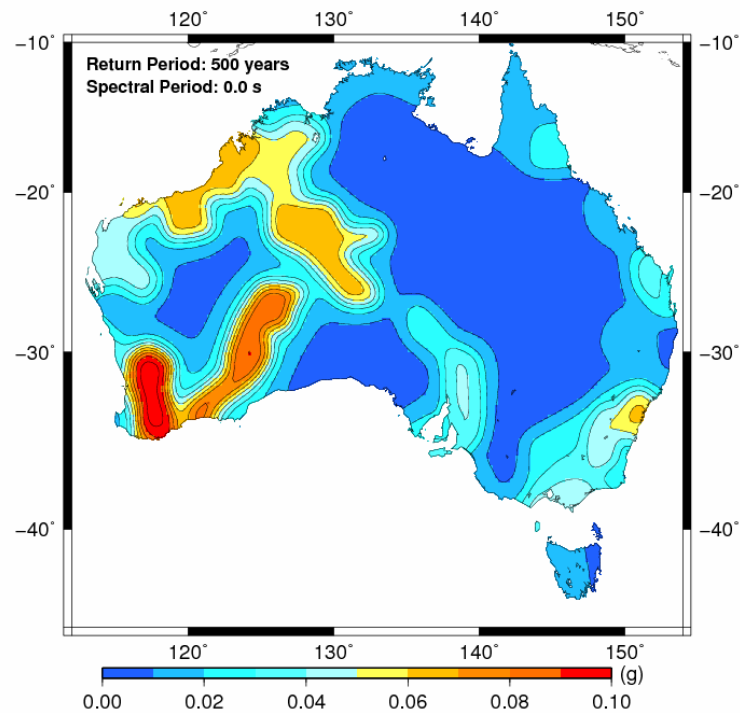


Figure 2 - The 500 year return period regional zone PGA (0.0 s RSA period) hazard map with a 300 km Gaussian spatial filter.

Hotspot Source Zones Only

Figure 3 shows the 500 yr, 0.0 s hazard for the hotspot zones only, smoothed this time with a 60 km width Gaussian filter. As described in Leonard *et al.* (this volume), the full catalogue was used (i.e. no declustering) and the maximum magnitude was reduced to 6.25 for all the hot spots. As one might expect, hazard values here are basically spikes centred on each hotspot.

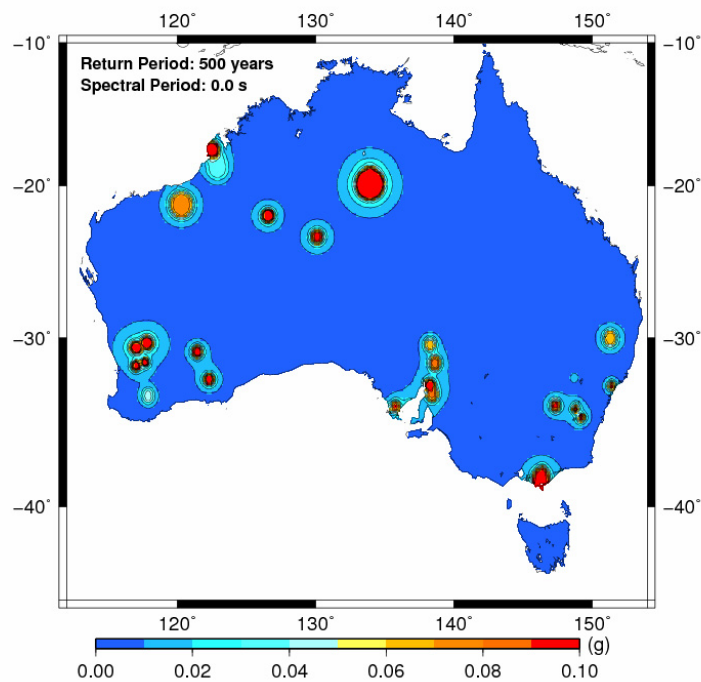


Figure 3 - The 500 year return period hotspot zone PGA (0.0 s RSA period) hazard map with a 60 km Gaussian spatial filter. Values above 0.1 g are shown in red.

Combined Hazard

There are a number of ways the hazard maps from each layer can be combined. One is to use the maximum hazard at each point from each layer, i.e. the worst case or maximum “credible” hazard from the three different models of seismic hazard shown previously. This means that the total integrated seismic moment across Australia is not conserved, but it allows the hazard in the areas of low seismic activity to be increased without decreasing the hazard in areas of high seismic activity. Figure 4a shows the 500 yr, 0.0 s hazard for the background, regional and hotspot hazard maps combined in this way. Each layer has been Gaussian filtered with the widths specified in the previous sections. Figure 4b shows the same map in 3D perspective to better illustrate the hazard values at the hotspots. Figure 5a & 5b show the 500 yr, PGA (0.0 s RSA period) hazard maps without the hotspot layer for comparison.

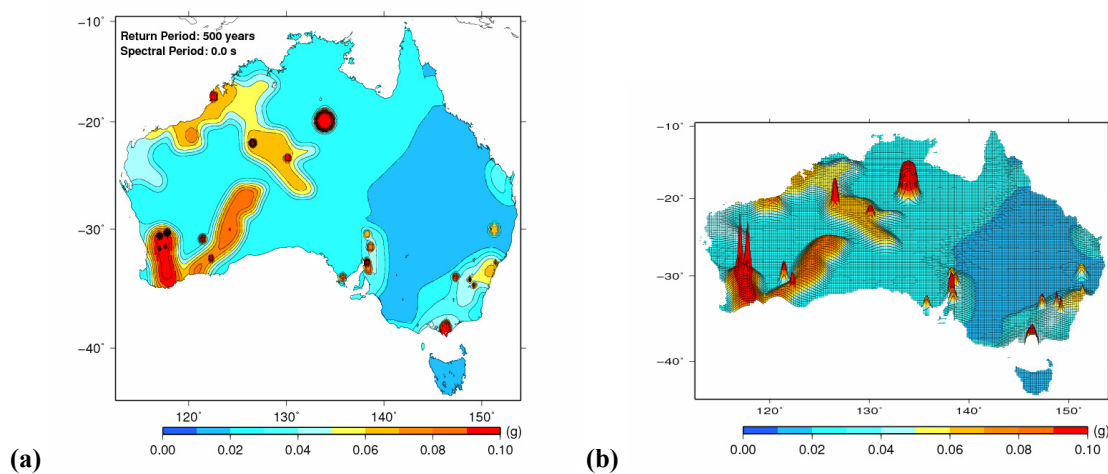


Figure 4 - The 500 year return period hotspot zone PGA (RSA 0.0 s period) hazard map calculated using the maximum hazard value for all three layers in (a) 2D and (b) 3D.

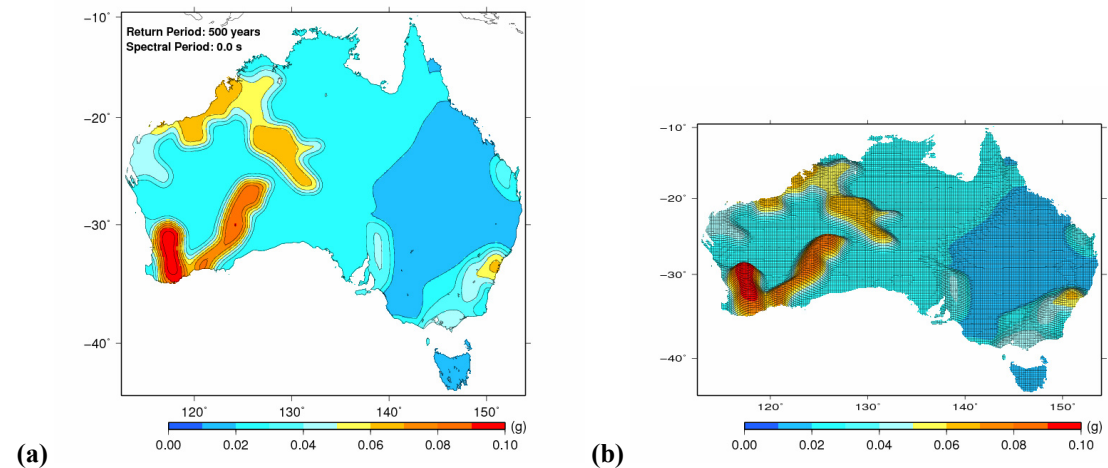


Figure 5 - The 500 year return period PGA (0.0 s RSA period) hazard map calculated using the maximum hazard value for the regional and background zone hazard maps only (i.e. no hotspots) in (a) 2D and (b) 3D.

Effect of the Gaussian width

Figure 6a demonstrates the effect of halving the width of the Gaussian filter on the regional source zone map. The effect is fairly small with only a small increase in detail (compare Figure

2 with Figure 6a). Figure 6b shows the hotspot zone map with the Gaussian spatial filter increased from 60 km to 300 km. In contrast the effect on the hotspot map is much more substantial. This is because the hotspots are spatial features much smaller than this Gaussian width (compare Figure 3 and Figure 6b).

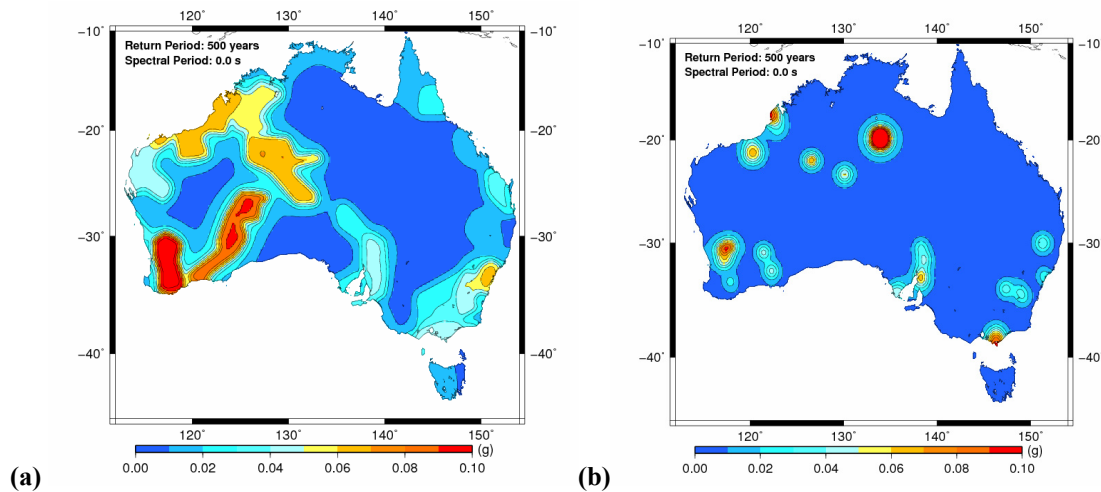


Figure 6 - The 500 year return period PGA hazard map for (a) the regional source zones with a 150 km Gaussian filter, and (b) the hotspot zones and a 300 km Gaussian filter.

The effect of using a 300 km Gaussian filter on the hotspot layer on the final hazard map is shown in Figure 7a and 7b. These maps should be compared to Figure 4 above. Most of the hot spot zones in Figure 4 produce hazard values less than the regional or background zones and thus don't appear in the maximum hazard map. Those that do appear (e.g. Tennant Creek) are smaller in amplitude but cover a slightly larger area.

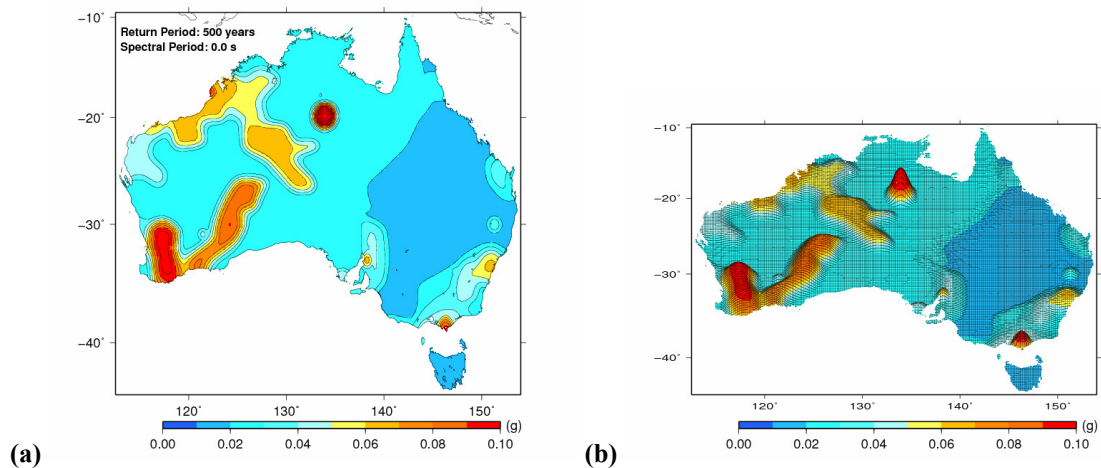


Figure 7 - The maximum hazard value for all three zones with the spatial filter width increased to 300 km for all layers in (a) 2D and (b) 3D.

Effect of return period

Figure 8 shows the national PGA hazard map at a range of other return periods. Naturally the level of hazard goes up as the return period increases. However, note that the rate of increase is slower for the hot spot zones (e.g. Tennant Creek) than it is for the regional zones. This is mostly due to the lower M_{max} values used in the hot spot layer zones (Leonard *et al.* this

volume). At 10,000 years the regional zones in WA have the largest earthquake hazard of any part of Australia.

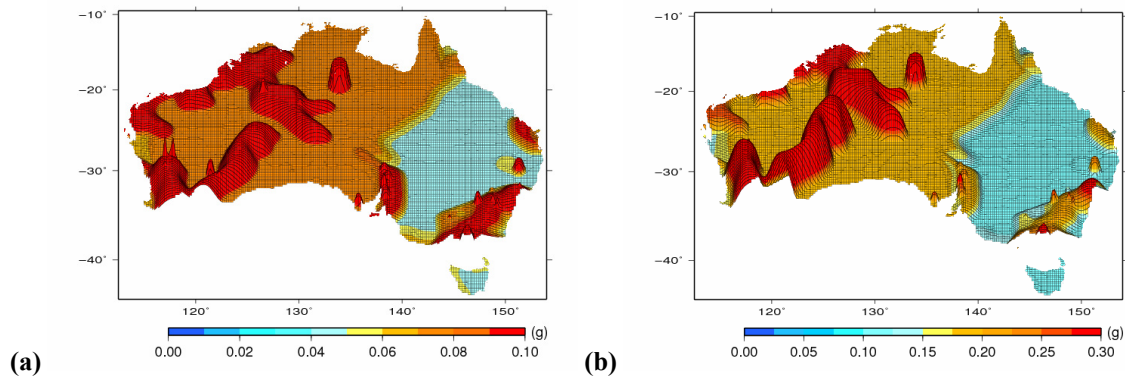


Figure 8 - The maximum hazard value for all three zones (Gaussian width 300 km for the background and regional zones, 60 km for the hot spot zones) for return periods of (a) 2475 years and (b) 10,000 years. Note that the colour scale in (b) and the vertical exaggeration in both (a) and (b) differs from the previous figures to prevent saturation.

Effect of spectral response period

Figure 9 shows the 500 year hazard map for two other spectral response periods (0.2 and 1.0 s) across the country. Hazard values for the 0.2 s map are consistently higher and, for the 1.0 s map, lower than the 0.0 s map right across Australia (compare Figure 4b to Figure 9a and b).

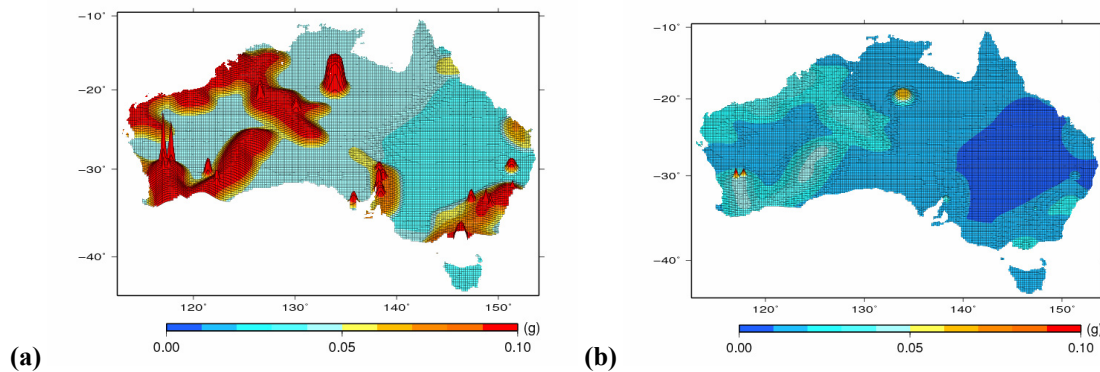


Figure 9 - The maximum hazard value for all three zones (Gaussian width 300 km for the background and regional zones, 60 km for the hot spot zones) for (a) 0.2 s RSA period and the (b) 1.0 s RSA period.

Figure 10a shows hazard at a specific point in Sydney as a function of return period for the three different response periods (the three solid lines). The hazard value was found by interpolating the hazard map using the GMT program “grdtrack”. Analogous figures for points in Melbourne, Brisbane and Perth are shown in Figure 10b-d. Also shown in Figure 10 are the PGA hazard values for hard rock calculated from Tables 3.1 and 3.2 in AS1170.4-2007 (the dashed red curve).

As can be seen, the hazard at the 0.2 s RSA period in the PSHA (blue solid curve) is higher than that for the 0.0 s RSA period hazard (solid red curve) and the 1.0 s hazard (green solid curve) for all the locations shown in Figure 10. The 0.0 s RSA hazard curves (red solid curve) produces hazard values in between the 0.2 s and 1.0 s RSA hazard curves (blue and green curves respectively). This is a direct result of the GMPE equations used in the draft map (Allen

et al. this volume). Naturally the hazard also increases as the return period increases, but starts to level off at the higher return periods.

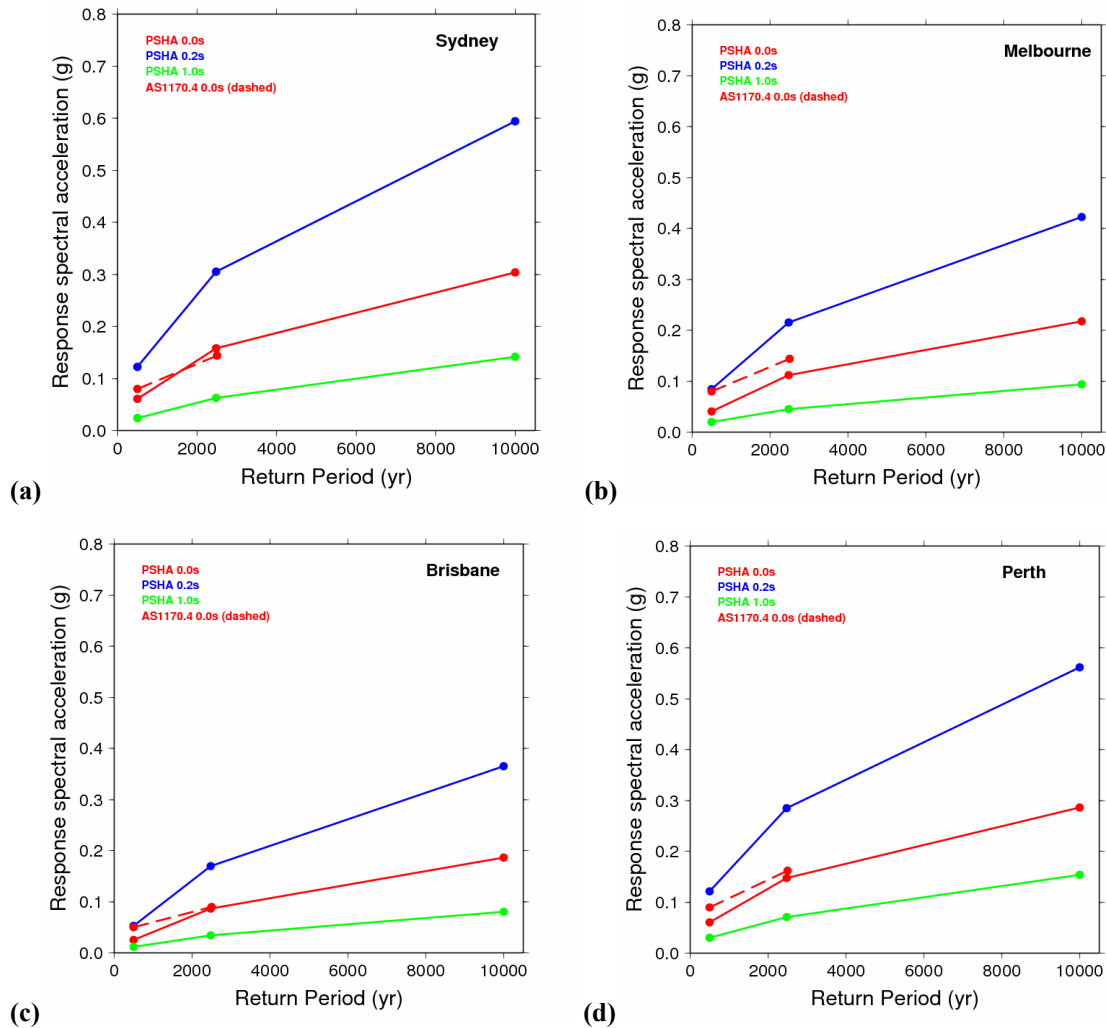


Figure 10 - Response spectral acceleration (Gaussian width 300 km for all layers) as a function of return period at three different spectral periods for locations in (a) Sydney, (b) Melbourne, (c) Brisbane and (d) Perth. The red, blue and green curves are the RSA values for 0.0 s, 0.2 s and 1.0 s from the draft probabilistic seismic hazard map. The red dashed curve is the 0.0 s hazard curve for these locations calculated using the tables in AS1170.4-2007.

For all the points considered here, the hazard factor (Z) in the current code (red dashed curve) is closest to either the 0.0 s or 0.2 s PSHA values (solid red and blue curves), depending on the location. The difference between Z and the PSHA values are typically <0.04 g for all of these particular locations. From a hazard assessment point of view, these differences are not very significant. Similarly, the hazard value for the point near Melbourne (Figure 10b) at 0.0 s, 500 years is close to the PGA hazard value determined for the Melbourne area by Brown & Gibson (2004).

Discussion

Uncertainties and limitations

The uncertainties in estimating the G-R recurrence parameters (a , b , M_{max}) are not included in these draft maps. In the case of the M_{max} parameter this will not significantly affect the 500 year return period map since all plausible values of M_{max} are above M7.0. Figure 11 shows the impact of changing M_{max} from 5.0 to 7.5 for Zone 11. As seen in the figure, increasing M_{max} from 5.0 to 7.0 nearly doubles the hazard, but changing it from 7.0 to 7.5 changes it by only by about 5%. This would be typical for most locations across Australia.

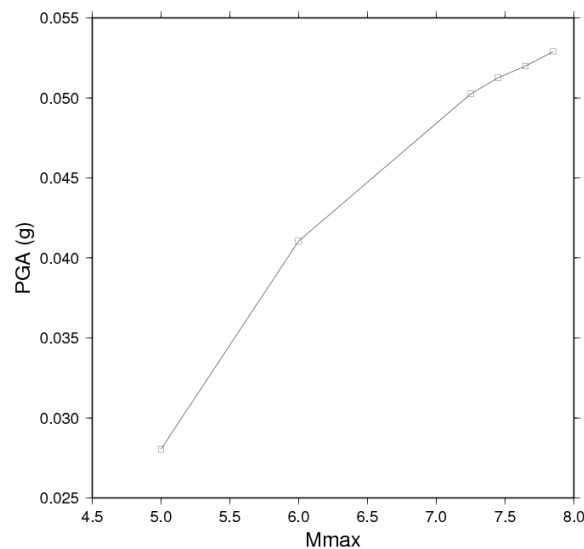


Figure 11 - The effect of changing the M_{max} variable on the hazard at a single location in Zone 11 (Victoria) at a return period of 500 years.

We have also assumed that there are no basin effects. In the multi-hazard assessment of Perth Sinadinovski *et al.* (2005) considered attenuation by the Perth Basin of short period seismic waves arriving from the craton to the east. This was based on very limited data. In the absence of sufficient new data to test this effect, we find it difficult to justify the application of this or any similar relation. Similarly, faults are not included as the data available to constrain the rates of fault motion are currently very limited. Furthermore, the effect on the hazard values from faults would generally be quite localised, and would most likely be removed by the smoothing required for a building code map.

Choice of map for AS1170.4

One of the key problems with the previous maps was that the hazard in areas with few earthquakes (e.g. Central Queensland) was low or zero. In the current AS1170.4-2007 map this was worked around by an expert committee smoothing previous hazard maps out into these areas using expert judgement. Here we extend the hazard out to these regions by using the background zones based purely on a simplified geological interpretation of Australia. This has the advantage that the hazard for the whole of Australia is now calculated probabilistically. It is also easy to update these background zones by simply including earthquakes as they happen and by modifying to the zone boundaries over time, as required. We recommend that this method is

adopted for the code map as the “floor”, or minimum, hazard value irrespective of any other maps that may be included.

The regional scale earthquake source zones have the advantage of more closely representing the observed distribution of seismicity without going into a high level of detail. This minimises the number of rapidly changing hazard values (i.e. steep contours) while still providing a more accurate representation of the distribution of seismicity at the regional scale relative to the background maps. The only areas where the hazard pattern (i.e. areas of high and low hazard) may change rapidly from version to version are near the edges of the zones. The advantage of this map over that currently utilised in AS1170.4-2007 is that the hazard is calculated fully probabilistically across a range of return and RSA periods, and can be updated in a straightforward manner as new information becomes available.

The hot spots zones represent small scale, often transient, variations in hazard across the continent much more accurately than the previous two layers. However, on a time scale of a decade or more many of these hotspots can be expected to change, with new ones needing to be added and inactive ones requiring removal. Accordingly, the hotspot layer will not necessarily remain stable from one edition of the map (and hence building code) to the next. In addition, the hotspot zones always produce very steep contours in the maps as they are quite small in area. Note that this would be an issue for any map with multiple small zones (e.g. Brown & Gibson 2004). Large amounts of smoothing can remove these steep contours, either by smoothing the initial seismicity (e.g. Hall *et al.* 2007) or by smoothing the final map. However, in both cases the effect of this would be to increase the hazard over a much larger area than that indicated by the distribution of seismicity. Geoscience Australia would welcome feedback from the Standards Australia committee regarding the inclusion or otherwise of hot spots in the AS1170.4 map.

Finally, there also remains the choice of which RSA and return period would be most suitable for the base map in the loading code. The simplest option would be to use a similar return period as that used in the current AS1170.4 map. This will keep changes in the “Z factor” in AS1170.4 to <0.04 g for the majority of the continent outside of the hot spots. The choice of the RSA period depends on which period is felt to best represent the ‘typical’ structure covered by the code. As discussed in McPherson *et al.* (this volume), the hazard factor, Z, does not have a well defined physical value (i.e. a response spectral period) but appears to be in the range of 0.0 to about 0.5 s (cf. Figure 10).

Other Applications of the Seismic Hazard Maps

While the main goal of these hazard maps is application under the Australian earthquake loading code (AS1170.4), they have a range of other potential uses, such as selecting scenarios for detailed hazard or risk assessments. A scenario seismic hazard or risk map shows the level of ground shaking or the impact from a specific earthquake. Many of the inputs to a scenario hazard/risk map are the same as for a probabilistic map, thus developments in one help the other. As previously mentioned EQRM produces a list of events as part of the process of calculating the hazard. Therefore, doing an assessment in this way makes it straight forward to disaggregate the hazard and select an event for a scenario hazard/risk assessment. Such maps are not used in the current standard, but have particular utility in scenario development to assist emergency managers with disaster response planning.

Conclusion

In this paper we have presented the draft results of a full probabilistic hazard assessment (PSHA) for Australia. As with most PSHAs, the result is a range of different hazard maps. These cover different choices of response spectral acceleration period, return period and earthquake recurrence model (from one with a high level of spatial detail which includes “hot spots” to one with a very low level of spatial detail). The results and method presented are based on the best available models and data for Australia, and have been designed to be flexible and easy to update. These models provide the ability to cover the full range of previous interpretations of the level of seismic hazard in Australia and should form an effective basis for future revisions of the hazard map underpinning the Australian earthquake loading code AS1170.4.

Acknowledgements

The authors would like to thank Andrew McPherson and Clive Collins for their thoughtful and constructive reviews of this manuscript. Generic Mapping Tools (Wessel and Smith, 1991) was used to generate the figures in this paper. We publish with the authorisation of the Chief Executive Officer of Geoscience Australia.

References

- Allen, T., Leonard, M. and Collins, C. (2011) The 2012 Australian Seismic Hazard Map – Catalogue and Ground Motion Prediction Equations. Proceedings of the 2011 Australian Earthquake Engineering Society Conference, Barossa Valley, SA (this volume).
- ATC (1984). *Tentative provisions for the development of seismic regulations for buildings, ATC 3-06 Amended*. Applied Technology Council, Redwood City, CA. 505 p.
- Burbidge, D. R., Allen, T. I., Leonard, M., McPherson, A. and Clark, D. (2011). *The 2012 Australian Earthquake Hazard Map - draft maps*. Proceedings of the 2011 Australian Earthquake Engineering Society Conference, Barossa Valley, SA (this volume).
- Brown, A. and Gibson, G. (2004). A multi-tiered earthquake hazard model for Australia, *Tectonophysics*, **390**, 25-43.
- Gaull, B.A., Michael-Leiba, M. O. & Rynn, J. M. W. (1990). Probabilistic earthquake risk maps of Australia. *Australian Journal of Earth Sciences* **37**, 169-187.
- Hall, L., Dimer, F. and Somerville, P. (2007). A Spatially Distributed Earthquake Source Model for Australia. Proceedings of the 2007 Australian Earthquake Engineering Society Conference, Wollongong, NSW.
- Leonard, M. (2010) Earthquake fault scaling; self-consistent relating of rupture length, width, average displacement, and moment release, BSSA, 100, 1971-1988.
- Leonard, M., Clark, D., Collins, C. & McPherson, A., The 2012 Australian Seismic Hazard Map – Source Zones and Parameterisation, Proceedings of the 2011 Australian Earthquake Engineering Society Conference, Barossa Valley, SA (this volume).

McCue, K. F. (1993) The revised Australian hazard map, 1991. Proceedings of the 1993 Australian Earthquake Engineering Society Conference, Sydney, NSW.

McPherson, A., Allen, T., Burbidge, D., Clark, D., Collins, C. and Leonard, M. (2011). The 2012 Australian Seismic Hazard Map - Introduction and Approach, Proceedings of the 2011 Australian Earthquake Engineering Society Conference, Barossa Valley, SA (this volume).

Sinadinovski C., Edwards M., Corby N., Milne M., Dale K., Dhu T., Jones A., McPherson A., Jones T., Gray D., Robinson D. and White J. (2005). Earthquake Risk. In: Jones, T. (ed.), *Natural hazard risk in Perth, Western Australia - Cities Project Perth Report*, GA Publication https://www.ga.gov.au/image_cache/GA6529.pdf

Robinson, D., G. Fulford, and T. Dhu (2005). EQRM: Geoscience Australia's Earthquake Risk Model: Technical manual: Version 3.0. *Geoscience Australia Record 2005/01*.

Robinson, D., Dhu, T. and Schneider, J. (2006). Practical probabilistic seismic risk analysis: A demonstration of capability, *Seismological Research Letters*, **77(4)**: 453-459.